GelBat: An Edible Gelatin-Based Battery

Hsing-Yu Chen[1,3], Alexander Keller[1,3], Andrew T. Conn[2,3] and Jonathan Rossiter[1,3]

***Abstract*— The development of green batteries has implications for many fields including sustainable robotics and edible electronics. Here we present GelBat, a biodegradable, digestible and rechargeable battery constructed from gelatin and activated carbon. The device utilises the water splitting reaction to produce a simple, sustainable Bacon fuel cell which can produce an output voltage of over 1V for 10 minutes, depending on the load resistance, with 10 minutes of charging and whose only byproduct is water. Electrochemical impedance spectroscopy, cyclic voltammetry and self discharge tests are carried out to characterize the behaviour of the battery. The system does not lose any efficiency with repeated recharging cycles and can be completely dissolved in a simulated gastric fluid within 20 minutes. The simplicity of this design combined with the bioresorbable materials demonstrates the potential of this work to help advance robotic research towards more sustainable untethered autonomous systems and edible robots.**

I. INTRODUCTION

The gastrointestinal (GI) tract is one of the most sophisticated, vital and fragile biological systems in nature. However, despite its importance we have yet to fully master effective means to both treat and monitor the health of the GI system. One of the primary reasons for the lack of effective GI medical options is that not only is it a complex synergistic system of organs, but its very nature is to break down materials for their conversion into chemical energy for the body, making long term survival of medical devices difficult [1]. As a result, traditional GI medical tools and treatments have been restricted to endoscopy [2], [3], laparoscopic surgery [4], [5], tomography [6], sonography [7], radiology [8], [9] and magnetic resonance imaging [10], [11]. Consequently, regular monitoring of the GI tract is rarely performed as these techniques are complicated, invasive, expensive and potentially dangerous. As a result, many medical issues that occur in the GI tract go undiagnosed and untreated until they become symptomatic leading to major healthcare challenges such as irritable bowel syndrome being undiagnosed in over 75% of US cases [12] and stomach cancer being the second leading cause of cancer related deaths globally [13].

Recently a new field of medical intervention known as electronic capsules has emerged in an attempt to allow for regular monitoring and treatment of the GI tract, which has been driven by the rapidly increasing miniaturization of electronics. This electronic miniaturization means that the sophisticated electronic components used to diagnose the GI system can now be fitted within the size of an ingestible capsule. These new medical devices are used to perform a range of functions in vivo, such as endoscopic monitoring [14], [15] and precision drug delivery [16], [17], as well and can form controllable and ingestible soft robotic devices [18], [19]. However, these electronic components are still constructed out of toxic materials and as such device retention is a major concern as fatalities occur in approximately 2% of all cases of ingestion of electronic capsules [20]. Consequently, electronic capsules are only used in limited circumstances and therefore for regular monitoring and treatment of the GI tract, new innovations need to be explored. One emerging field of research which seeks to produce medical tools that can be used regularly for GI diagnosis is known as edible electronics.

Edible electronics, which are a type of bioelectronics, seek to produce medical devices which can be used to treat and monitor the GI system but without the traditional concerns of toxicity, infection and immunogenicity as the components used to construct the electronics are sourced from digestible materials [21], [22]. Although this is a nascent field, many different edible devices have been demonstrated, such as sensors [23], [24], tissue stimulants [25], super capacitors [26] and actuators [27], [28]. However, one of the most vital developments needed to help further the state-of-the-art of bioelectronic research is the production of digestible batteries. Inherently soft and compliant digestible batteries offer better mechanical interactions with the GI tract, while also having the potential to support advances towards the next generation of untethered autonomous robots which embody their energy storage [29]. Herein we present a method for the construction of a simple, soft, rechargeable, edible battery called GelBat (Figure 1(a,b)), using the abundant biomaterials gelatin and activated carbon to hopefully help further not only the field of edible robotics but the entire field of bioelectronics.

II. FABRICATION

The edible battery is simply composed of two ingredients: gelatin and activated carbon, due to their biocompatibility and bioabsorbility. Activated charcoal was used as it is not only an edible conductor (E-number: E153) but its high surface area is commercially used as a substrate to adsorb intestinal gases as a treatment for stomach bloating. It was therefore proposed that this material could not only act as an inert electrode to split water but that the produced gases would then be contained within these high surface area electrodes ready to be recombined when discharging. Firstly,

Corresponding author: hsing-yu.chen@bristol.ac.uk

[1]Department of Engineering Mathematics, University of Bristol, UK

[2]Department of Mechanical Engineering, University of Bristol, UK

[3]SoftLab, Bristol Robotics Laboratory, University of Bristol and University of the West of England, UK

Data supporting this work can be accessed at: doi.org/10.5523/bris.2c4017s8543i2od5qdx3osoqd

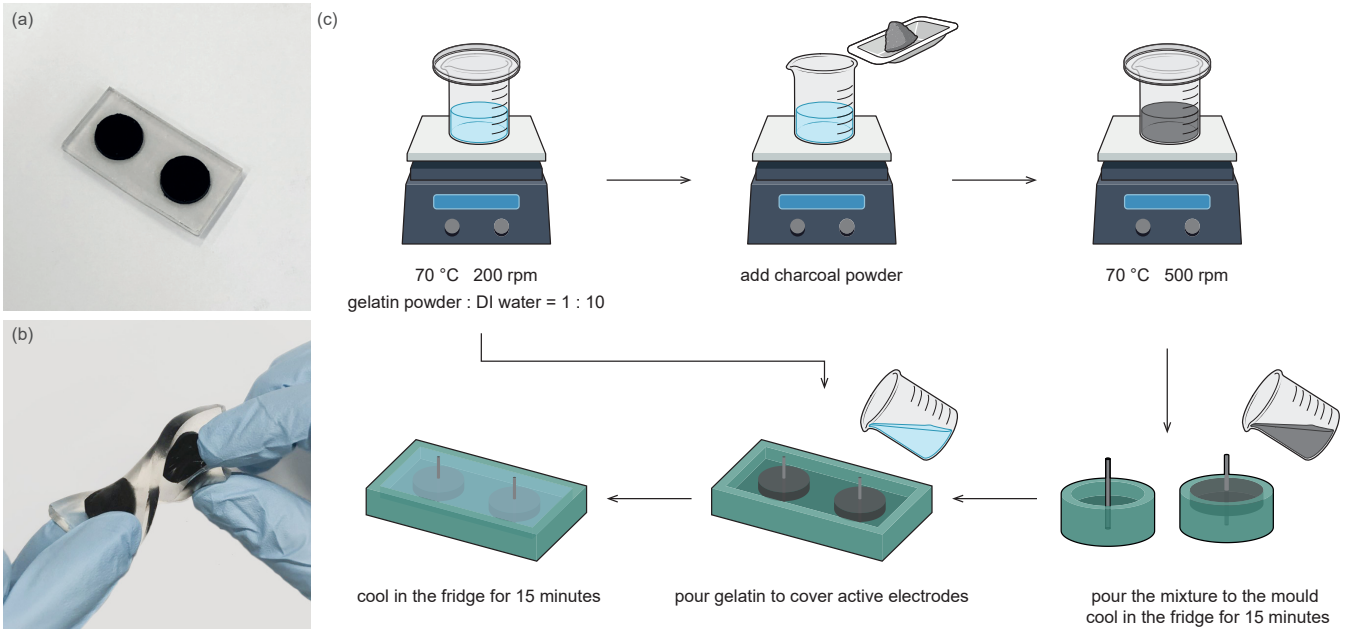

Fig. 1. (a) The photo of GelBat, which is consisted of gelatin and activated carbon. (b) The GelBat itself is flexible and compliant. (c) The fabrication process of making GelBat.

the gelatin solution is prepared by dissolving the dehydrated powder (CAS: 9000-70-8, Sigma-Aldrich) into deionised water with a ratio of 1:10, followed by a heating and stirring treatment at 70 °C and 200 rpm until it is completely dissolved. To prevent contamination and content loss, the beaker is covered with a lid during the entire process. The conductivity of the electrodes is achieved by adding activated carbon powder (CAS: 7440-44-0, Sigma-Aldrich) into the solution with a designated ratio at the same temperature but the stirrer speed is further escalated to 500 rpm to account for the increased viscosity. The fluid is poured into a SLA-printed mould with a diameter of 15 mm and thickness of 3 mm and a 0.7 mm graphite rod from a pencil with 15 mm long is held in the middle of the mould for further electrical connection. After being covered and cooled in the fridge, the cured electrode disks are transferred to another rectangular mould featured by 50 mm × 25 mm and submerged in pure aqueous gelatin obtained by aforementioned approach. The complete fabrication process is illustrated in Figure 1(c).

III. Working Principle

The device works via the exploitation of the water splitting reaction described in equation 1:

$$2H_2O_{(l)} \rightleftharpoons 2H_{2(g)} + O_{2(g)} \qquad E^\circ = 1.23V \qquad (1)$$

First a potential difference is applied between the two carbon electrodes with a potential difference greater than that of the theoretical standard electrode potential of the redox reaction of water (>1.23 V). This produces adsorbed oxygen gas at one electrode and hydrogen gas at the opposite electrode via the water splitting reaction described above. The oxygen and hydrogen gas adsorbed to the activated carbon surfaces can then spontaneously recombine when the circuit is complete, according to equation 1, generating a voltage. This process can be repeated an infinite number of times as long as there is available water.

IV. Characterisations

A. Concentration of Activated Carbon

To evaluate the contribution of activate carbon to electrochemical response, the electrodes are formed by three different ratios of activated carbon and gelatin of 1:10, 1:30 and 1:50 while the concentration of gelatin is fixed at 10% weight by volume. A pristine gelatin without conductive carbon material is also investigated to understand the effect of surface area from that of electrode composition. The characteristics of the charging and discharging performance are assessed by connecting the battery to known resistors in series and the switch between the states is controlled by a relay via a custom script as illustrated in Figure 2(a). The electric potential across the resistors is monitored by a data acquisition device (DAQ, USB-6001, National Instruments) so that the current flowing in and out the battery can be obtained by Ohm's law.

Figure 2(b) shows the voltage across the battery for the first five charging and discharging cycles out of ten. For charging, the capacitor is gradually charged up through a 120 Ω resistor from a continuous 5 V power source for 10 minutes. As the order of the selected resistor, 120 Ω, is not much larger than that of the capacitance of the battery, the resultant small RC time constant makes the transient response indiscernible in the graph. Whilst for discharging, the charged capacitor is disconnected from the DC supply voltage and the stored energy is released through a 1 MΩ resistor for another 10 minutes. As shown in the figure, the voltage substantially drops at the start but then tapers

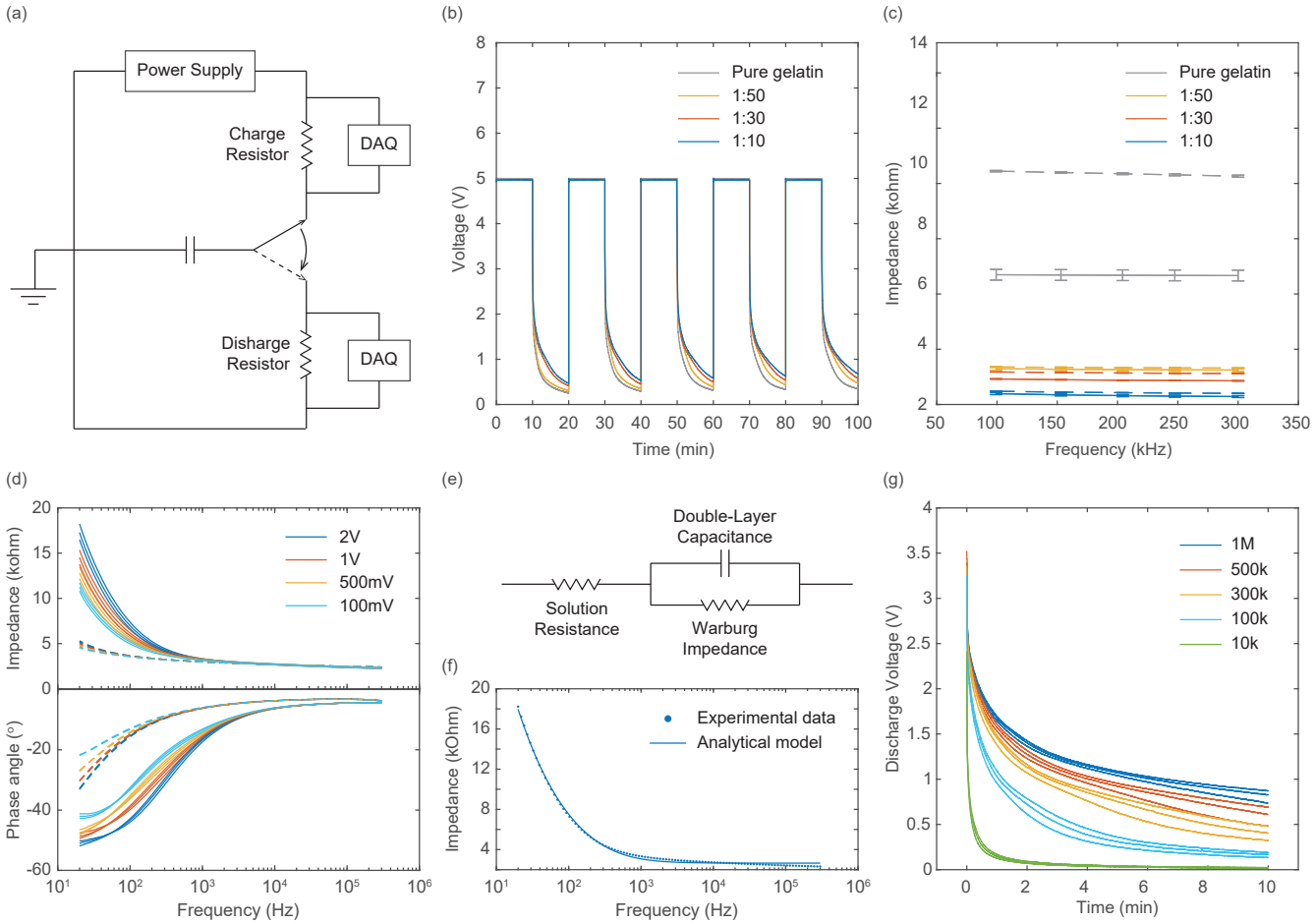

Fig. 2. (a) An illustration of the electrical circuit used to measure the charing and discharging behaviours. (b) The investigation of various ratio of electrodes by charging 10 minutes through a 120 Ω resistor at 5 V and discharging 10 minutes through a 1 MΩ load resistor. The entire experiment is cycled 10 times and here the first 5 cycles are shown. (c) The comparisons of different concentrations of electrodes excited by 100 mV at high frequencies where the contribution of impedance from diffusion and electrolysis can be negligible. (d) The electrochemical impedance spectrum for 1:10 ratio with various excitation levels. (In (c) and (d), the solid and dashed lines are the impedance variance before and after 10 charging and discharging cycles resulting from (b).) (e) The electrochemical behaviour can be modelled by a simplified Randles circuit. (f) The Bode plot of analytical model and experimental data. The dotted line is the measured impedance spectrum of ratio 1:10 excited with 100 mV and the solid line is the fitting result with R_s = 2.65 kΩ, C_{dl} = 691.3 nF and α = 87.9 kΩ s$^{-1/2}$ (g) The discharging profiles through various load resistors after charging for 10 minutes at 5 V.

off exponentially at a slower rate. This is proposed to be a result of the initial voltage being a combination of the discharge from the built-up capacitance of the system and the electrochemical recombination of oxygen and hydrogen. Consequently, as can be seen in the figure, once all the capacitance has been discharged a plateau region of the generated voltage is observed. This phenomenon is the electrochemical energy generated from the recombination of the stored oxygen and hydrogen becoming the dominate driving force of the voltage. It is found that the composites with higher concentration of conductive carbon powder have larger time constant and lose charge at a slower rate, thereby being able to maintain slightly higher voltage after the same amount of discharging time.

B. Electrochemical Impedance Spectroscopy

The electrochemical impedance spectroscopy (EIS) is conducted to analyze the interfacial properties at the electrode surface and the electrolyte in response to different electrical conditions. Two ends of the electrodes are connected to a LCR meter (E4980AL, Keysight) and their electrical impedance is measured by sweeping over a wide range of frequencies from 20 Hz to 300 kHz.

As ionic conductivity is diffusion driven, the resistive component of the impedance can be isolated by running impedance measurements at high frequencies (<100 kHz) and low excitation level (100 mV), making the contribution of impedance from diffusion and electrolysis negligible. Figure 2(c) presents the magnitude of impedance for each ratio of electrode at high frequencies as this is the region where the mobility of diffusing reactants is reduced and the impedance is predominately caused by ohmic resistance of the electrolyte. There is a notable discrepancy between pristine gelatin substrates and those introduced with augmented electrodes, implying that adding activated carbon has a considerable improvement on conductivity. The averages of the impedance at high frequencies are 6.7 kΩ for pure

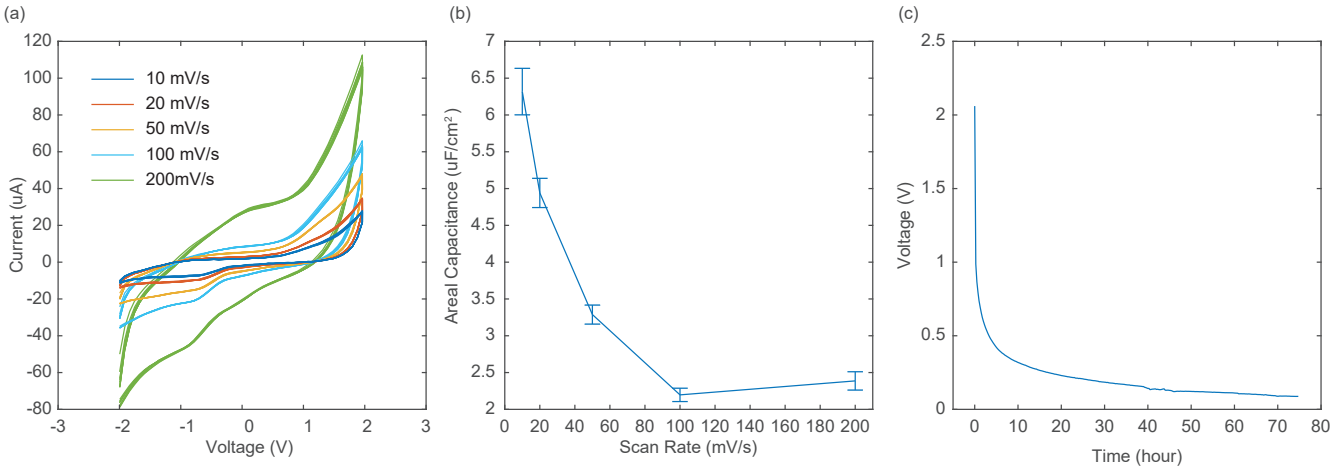

Fig. 3. (a) The voltage-current relationship of the electorchemical cell when the voltage is swept between −2 V and 2 V at various scan rates. (b) Scan rate dependent areal capacitance plot. (c) Self-discharge curve over 3 days after 1 hour of 5 V charging.

gelatin and 3.3 kΩ, 2.9 kΩ and 2.3 kΩ for increased charcoal concentrations of 1:50, 1:30 and 1:10 respectively. This result has consistent correspondence with the discharging curve appearing in Figure 2(b) that higher density of reactive component exhibits a high electrochemical performance and therefore a better option for micro energy storage devices.

Figure 2(d) shows the EIS spectrum of electrode ratio 1:10 with various excitation level (V∈ [100 mV, 500 mV, 1 V, 2 V]) by Bode plots, in which the impedance magnitude and phase angle are plotted against the logarithm of the frequency. The plot can be divided into two regions. At low frequencies, the impedance is attributed by both capacitor and electrolyte. With increasing frequency, the impact from the capacitor is damped out, showing the real impedance of the solution. In Figure 2(c) and (d), the solid and dashed lines are the impedance variance before and after 10 charging and discharging cycles. The impedance is significantly decreased at low frequencies and slightly increased at high frequencies. This is suggested to be a result of the electrochemical behaviour switching to becoming dominated by the recombination of oxygen and hydrogen over diffusion as more cycles are performed. This may be a consequence of more efficient pathways of oxygen and hydrogen reforming being established as more cycles are performed allowing for both easier water splitting and recombination.

The internal impedance of GelBat can be approximated as a simplified Randles circuit, which consists of a resistance (R_s) in series with the parallel of double layer capacitance (C_{dl}) and Warburg impedance (Z_W) as illustrated in Figure 2(e). In this proposed equivalent electrochemical model, R_s represents the solution resistance when ions transfer from one electrode to another, C_{dl} is associated with behaviour at the interface between two electrodes and the adjacent electrolyte and Z_W is used to characterise the chemical diffusion process. As both double-layer capacitance and Warburg impedance are dependent on frequency, more current will flow through the path with the less resistance. The equivalent impedance can be expressed by equation 2, where ω is angular frequency, j is the imaginary unit and Warburg impedance, Z_W, is defined as $\alpha/\sqrt{j\omega}$, where α is Warburg coefficient.

$$Z_{eq} = R_s + \frac{1}{\frac{1}{Z_w} + \frac{1}{j\omega C_{dl}}} \tag{2}$$

As shown in Figure 2(f), the dotted line is the measured impedance spectrum of ratio 1:10 excited with 100 mV while the solid line is the fitted curve with $R_s = 2.65 \pm 0.32\,\text{k}\Omega$, $C_{dl} = 691.3 \pm 30.5\,\text{nF}$ and $\alpha = 87.9 \pm 1.5\,\text{k}\Omega\,\text{s}^{-1/2}$. It is shown that the experimental data can be well represented by equivalent circuit with $R^2 = 0.9978$.

C. Load Effect

Characterisation of the load effect on discharge profile is performed by the same set up illustrated in Figure 2(a) and the same method described in section IV-A while the discharging load resistors varied from 10 kΩ, 100 kΩ, 300 kΩ, 500 kΩ to 1 MΩ. As can be seen in Figure 2(g), the rate of discharge of the sample is highly dependent on the resistor that it is connected in series with as illustrated by the sample connected to a 10 kΩ resistor discharging within 10 minutes, whereas the sample connected to a 1 MΩ resistor was still generating 1V after 10 minutes. Therefore, these results highlight that the choice of resistor which is to be integrated into the device has to be carefully selected for purpose. For example, if a fast discharge or quick response is required for an application such as an electrochemically induced drug release, a small resistor should be connected to the sample. However, if a prolonged operation is required for an application such as health monitoring a larger resistor should be connected to the system. This work therefore demonstrates the ease of tailoring the discharge rate and duration of operation of this edible battery via the selection of the resistor.

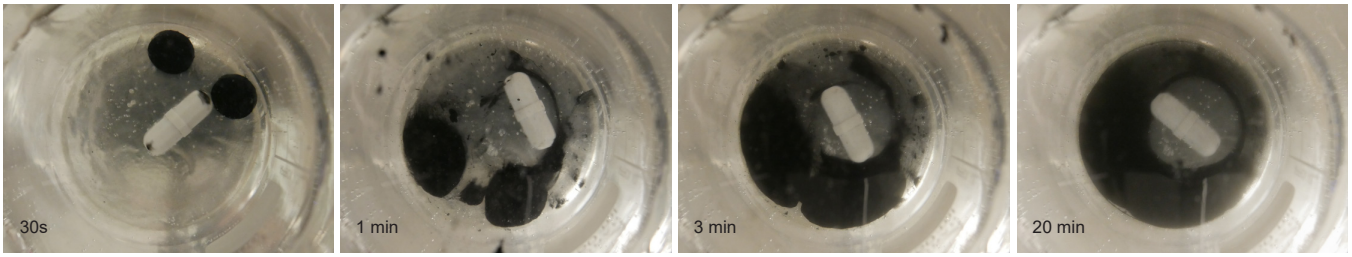

Fig. 4. The sequential images of dissolving GelBat in simulated gastric solution.

D. Cyclic Voltammetry

To investigate the current response subject to Faradaic and non-Faradaic processes, cyclic voltammetry (CV) is carried out by linearly ramping up and down the voltage between two vertex potentials. Figure 3(a) shows the resulting cyclic voltammogram scanning from -2 V to 2 V at 5 different scan rates, $\upsilon \in$ [10, 20, 50, 100, 200] mV s^{-1}, for 10 times in a two-electrode configuration at ambient temperature. It is observed that faster scan rates lead to higher currents. This is proposed to be an effect of a decrease in the size of the diffusion layer and as a consequence, higher currents are observed. The areal specific capacitance, C_A, can be obtained from equation 3, where V_1 and V_2 are the lower and upper bounds of the potential window, A is the surface area of electrodes, υ is the scan rate and the integration of the CV profile is the amount of charge being transferred during the electro-chemical process.

$$C_A = \frac{1}{2(V_2 - V_1)A\upsilon} \int_{V_1}^{V_2} i\,dt \tag{3}$$

In Figure 3(b), it is shown that the specific capacitance is scan-rate dependent. This could be explained by the kinetics of electrochemical reactions as faradaic current has time to transit in the electrolyte at slower scan rates when oxidation–reduction reactions occur, therefore increasing the capacitance. It is worth noting the cell exhibited stable cyclic performance as the areal specific capacitance remained essentially stable among 80 cycles with only 7% variance.

E. Self-Discharge

It is also important to examine how well the initial energy is preserved with regard to self-discharge behavior as the spontaneous chemical reaction could slowly occur and reduce the stored energy even when there is no connection to external circuits. To measure the voltage drop due to self-discharge instead of depleting through internal resistance of the measuring device, the GelBat is connected to a relay so that the circuit remains continuously unloaded and only closed once every 15 minutes for a 0.5 second long measurement. After being charged for an hour, the voltage dropped from 2.06 V and asymptotically reduced to 111 mV after 60 hours, leading to a self-discharge rate of 32.5 mV h^{-1} as shown in Figure 3(c). This is possibly due to the fact that the gas cannot be fully captured in the gelatin substrate, the porosity of which can be improved by increasing gelatin concentration in the future.

F. Digestibility

As the GelBat is solely composed of edible materials, gelatin and activated carbon, the dissolvability in an acidic fluid was carried out. The simulated gastric fluid was prepared by dissolving 500 mg $NaCl_2$ into 250 mL deionised water and tailoring the pH value to 1.2 with HCl solution. The fluid is incubated in a 37 °C water bath with a magnetic stirring bar at 50 rpm to emulate a stomach environment. Figure 4 presents a series of time-lapsed shots after displacing the GelBat into the simulated gastric solution. It shows that the GelBat can be completely discomposed within 20 minutes.

V. DISCUSSION AND CONCLUSIONS

The development of green electronics which are both biodegradable and bioresorbable can not only help the progress of sustainable robotics but help produce new paradigms in healthcare. To help advance the state-of-the-art of this field of research a biodegradable, digestible, rechargeable battery constructed of biomaterials gelatin and activated carbon is developed. The device is shown to produce an output voltage of over 1 V through 1 MΩ for 10 minutes with 10 minutes of 5 V charging. Furthermore, the system does not appear to lose any efficiency after 80 recharging cycles and can disintegrate in a simulated gastric environment after 20 minutes. The simplicity of this design, its edible components, environmentally and biological compatible byproducts and recharging efficiency demonstrates the potential that this research has to aid in the progress of edible and green robotics research.

Typical edible batteries in the literature require metals to be consumed, which not only have safety implications when consumed in modest quantities but also produce potentially harmful byproducts. In contrast, the byproducts of the chemical recombination reaction in the GelBat is exclusively water, eliminating any concerns about toxicity. Furthermore, in future multiple GelBats could be safely combined to increase the energy output. Alternative capacitive edible batteries have been presented, but these require complex manufacturing and limited material choices, such as fish melanin, which can exclude people with dietary restrictions, such as allergies, religious concerns and vegetarianism. The simplicity of our design allows the versatility of material to be tailored towards the users and lower the barrier of access to this technology. Although the current design is not optimised for

oral administering, preliminary investigations have revealed that the redesign of the geometry into a tablet form can be easily achieved. The development and characterisation of a smaller GelBat tablet will be explored in future studies.

ACKNOWLEDGMENT

This work was supported by Engineering and Physical Sciences Research Council (EPSRC) grant EP/R02961X/1. J.R. was also supported by EPSRC grants EP/S021795/1, EP/V026518/1, EP/V062158/1, EP/T020792/1 and EP/S026096/1, and the Royal Academy of Engineering through the Chair in Emerging Technologies scheme, CiET1718/22. AK is also supported by EU Horizon 2020 grant ROBOFOOD (964596).

REFERENCES

[1] S. J. Mulvihill and H. T. Debas, "History of surgery of the gastrointestinal tract," in *Surgery*. Springer, 2001, pp. 399–412.

[2] H. K. Chung and J. R. Lightdale, "Sedation and monitoring in the pediatric patient during gastrointestinal endoscopy," *Gastrointestinal Endoscopy Clinics*, vol. 26, no. 3, pp. 507–525, 2016.

[3] J. L. Achord and V. R. Muthusamy, "The history of gastrointestinal endoscopy," in *Clinical gastrointestinal endoscopy*. Elsevier, 2019, pp. 2–11.

[4] G. Liao, S. Wen, X. Xie, and Q. Wu, "Laparoscopic gastrectomy for remnant gastric cancer: Risk factors associated with conversion and a systematic analysis of literature," *International Journal of Surgery*, vol. 34, pp. 17–22, 2016.

[5] A. Gangemi, S. Russel, K. Patel, H. Khalaf, M. Masrur, and C. Hassan, "Conversion to laparoscopic sleeve gastrectomy after failure of laparoscopic gastric band: a systematic review of the literature and cost considerations," *Obesity Research & Clinical Practice*, vol. 12, no. 5, pp. 416–420, 2018.

[6] K. P. Banks and W. S. Song, "Role of positron emission tomography–computed tomography in gastrointestinal malignancies," *Radiologic Clinics*, vol. 51, no. 5, pp. 799–831, 2013.

[7] S. Parangi, D. Levine, A. Henry, N. Isakovich, and S. Pories, "Surgical gastrointestinal disorders during pregnancy," *The American journal of surgery*, vol. 193, no. 2, pp. 223–232, 2007.

[8] S. Azeze, S. Rahim, A. Sands, J. Shrewsbury, and S. Tavri, "The role of interventional radiology in the management of acute gastrointestinal bleeding," *Journal of Radiology Nursing*, vol. 37, no. 3, pp. 188–197, 2018.

[9] D. Sudheendra, A. C. Venbrux, A. Noor, A. K. Chun, S. N. Sarin, A. S. Akman, and E. K. Jackson, "Radiologic techniques and effectiveness of angiography to diagnose and treat acute upper gastrointestinal bleeding," *Gastrointestinal Endoscopy Clinics*, vol. 21, no. 4, pp. 697–705, 2011.

[10] F. Varyani and S. Samuel, "Can magnetic resonance enterography (mre) replace ileo-colonoscopy for evaluating disease activity in crohn's disease?" *Best Practice & Research Clinical Gastroenterology*, vol. 38, p. 101621, 2019.

[11] G. Khatri, J. Coleman, and J. R. Leyendecker, "Magnetic resonance enterography for inflammatory and noninflammatory conditions of the small bowel," *Radiologic Clinics*, vol. 56, no. 5, pp. 671–689, 2018.

[12] A. Hungin, L. Chang, G. Locke, E. Dennis, and V. Barghout, "Irritable bowel syndrome in the united states: prevalence, symptom patterns and impact," *Alimentary pharmacology & therapeutics*, vol. 21, no. 11, pp. 1365–1375, 2005.

[13] J. Ferlay, H.-R. Shin, F. Bray, D. Forman, C. Mathers, and D. M. Parkin, "Estimates of worldwide burden of cancer in 2008: Globocan 2008," *International journal of cancer*, vol. 127, no. 12, pp. 2893–2917, 2010.

[14] G. Ciuti, R. Caliò, D. Camboni, L. Neri, F. Bianchi, A. Arezzo, A. Koulaouzidis, S. Schostek, D. Stoyanov, C. Oddo *et al.*, "Frontiers of robotic endoscopic capsules: a review," *Journal of micro-bio robotics*, vol. 11, no. 1, pp. 1–18, 2016.

[15] C. K. Sorrell, S. Rajan, and T. N. Lunsford, "Role of capsule endoscopy and device-assisted enteroscopy in the management of patients hospitalized with gastrointestinal bleeding," *Hospital Medicine Clinics*, vol. 1, no. 2, pp. e72–e90, 2013.

[16] Y. Zhuang, W. Hou, X. Zheng, Z. Wang, J. Zheng, X. Pi, J. Cui, Y. Jiang, S. Qian, and C. Peng, "A mems-based electronic capsule for time controlled drug delivery in the alimentary canal," *Sensors and Actuators A: Physical*, vol. 169, no. 1, pp. 211–216, 2011.

[17] P. J. van der Schaar, J. F. Dijksman, H. Broekhuizen-de Gast, J. Shimizu, N. van Lelyveld, H. Zou, V. Iordanov, C. Wanke, and P. D. Siersema, "A novel ingestible electronic drug delivery and monitoring device," *Gastrointestinal endoscopy*, vol. 78, no. 3, pp. 520–528, 2013.

[18] P. Cortegoso Valdivia, A. R. Robertson, N. K. De Boer, W. Marlicz, and A. Koulaouzidis, "An overview of robotic capsules for drug delivery to the gastrointestinal tract," *Journal of Clinical Medicine*, vol. 10, no. 24, p. 5791, 2021.

[19] M. R. Basar, F. Malek, K. M. Juni, M. S. Idris, and M. I. M. Saleh, "Ingestible wireless capsule technology: A review of development and future indication," *International Journal of Antennas and Propagation*, vol. 2012, 2012.

[20] E. Rondonotti, J. M. Herrerias, M. Pennazio, A. Caunedo, M. Mascarenhas-Saraiva, and R. de Franchis, "Complications, limitations, and failures of capsule endoscopy: a review of 733 cases," *Gastrointestinal endoscopy*, vol. 62, no. 5, pp. 712–716, 2005.

[21] A. Keller *et al.*, "Printed organic electronic device components from edible materials," *MRS Online Proceedings Library (OPL)*, vol. 1717, 2015.

[22] Y. J. Kim, S.-E. Chun, J. Whitacre, and C. J. Bettinger, "Self-deployable current sources fabricated from edible materials," *Journal of Materials Chemistry B*, vol. 1, no. 31, pp. 3781–3788, 2013.

[23] C. J. Bettinger, "Edible hybrid microbial-electronic sensors for bleeding detection and beyond," *Hepatobiliary Surgery and Nutrition*, vol. 8, no. 2, p. 157, 2019.

[24] A. Keller, J. Pham, H. Warren *et al.*, "Conducting hydrogels for edible electrodes," *Journal of Materials Chemistry B*, vol. 5, no. 27, pp. 5318–5328, 2017.

[25] J. Koo, M. R. MacEwan, S.-K. Kang, S. M. Won, M. Stephen, P. Gamble, Z. Xie, Y. Yan, Y.-Y. Chen, J. Shin *et al.*, "Wireless bioresorbable electronic system enables sustained nonpharmacological neuroregenerative therapy," *Nature medicine*, vol. 24, no. 12, pp. 1830–1836, 2018.

[26] X. Wang, W. Xu, P. Chatterjee, C. Lv, J. Popovich, Z. Song, L. Dai, M. Y. S. Kalani, S. E. Haydel, and H. Jiang, "Food-materials-based edible supercapacitors," *Advanced Materials Technologies*, vol. 1, no. 3, p. 1600059, 2016.

[27] S. Zhang, A. M. Bellinger, D. L. Glettig, R. Barman, Y.-A. L. Lee, J. Zhu, C. Cleveland, V. A. Montgomery, L. Gu, L. D. Nash *et al.*, "A ph-responsive supramolecular polymer gel as an enteric elastomer for use in gastric devices," *Nature materials*, vol. 14, no. 10, pp. 1065–1071, 2015.

[28] C. J. Bettinger, "Advances in materials and structures for ingestible electromechanical medical devices," *Angewandte Chemie International Edition*, vol. 57, no. 52, pp. 16 946–16 958, 2018.

[29] C. A. Aubin, B. Gorissen, E. Milana, P. R. Buskohl, N. Lazarus, G. A. Slipher, C. Keplinger, J. Bongard, F. Iida, J. A. Lewis, and R. F. Shepherd, "Towards enduring autonomous robots via embodied energy," *Nature*, vol. 602, pp. 393–402, 2022.